

NOTE

Light propagation in dentin: influence of microstructure on anisotropy

Alwin Kienle, Florian K Forster, Rolf Diebold and Raimund Hibst

Institut für Lasertechnologien in der Medizin und Meßtechnik, Helmholtzstr. 12,
D-89081 Ulm, Germany

E-mail: alwin.kienle@ilm.uni-ulm.de

Received 17 September 2002, in final form 8 November 2002

Published 23 December 2002

Online at stacks.iop.org/PMB/48/N7

Abstract

We investigated the dependence of light propagation in human dentin on its microstructure. The main scatterers in dentin are the tubules, the shape of which can be approximated as long cylinders. We calculated the scattering of electromagnetic waves by an infinitely long cylinder and applied the results in a Monte Carlo code that simulates the light propagation in a dentin slab considering multi-scattering. The theory was compared with goniometric measurements. A pronounced anisotropic scattering pattern was found experimentally and theoretically. In addition, intensity peaks were measured which are shown to be caused by light diffraction by the tubules.

(Some figures in this article are in colour only in the electronic version)

For diagnostic applications of light in medicine it is important to understand the influence of the tissue's microstructure on light propagation. This knowledge enables early detection of structural tissue alterations, which strongly increases the probability of successful treatment. In the literature the dependence of light propagation on the microstructure has been studied on cells (Mourant *et al* 2002, Drezek *et al* 1999, Beuthan *et al* 1996), but very few successful investigations have been made on larger tissue volumes (Perelman *et al* 1999, Backman *et al* 2000). In addition, for the applied models it was assumed that light propagation is isotropic, i.e. that the optical properties do not depend on the photons' direction. However, this is not true for many tissue types, for example, muscle, ligament, tendon, skin, enamel and dentin. Anisotropic light propagation in these tissues is caused by their aligned (cylindrical) microstructure.

In this study we show that light propagation in dentin, the bone-like part of the tooth, can be successfully explained by its microstructure and that light propagation is considerably anisotropic. The main scatterers in dentin are the tubules (Zijp and ten Bosch 1993), which serve as supply channels for the metabolism of the organic matrix of dentin. As shown in figure 1(a), the tubules extend from the pulp to the enamel–dentin junction. To visualize the three-dimensional arrangement of the tubules, we performed measurements on human dentin

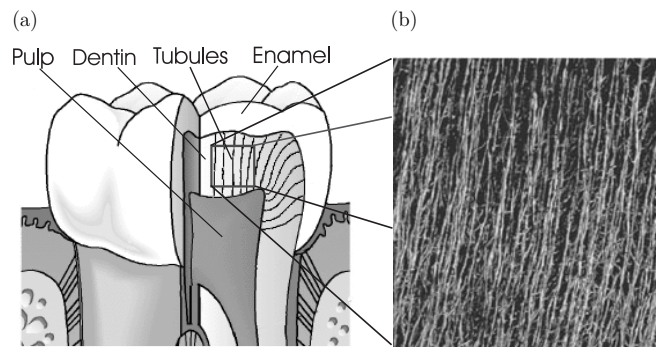


Figure 1. (a) Scheme of the tooth including dental tubules. (b) LSM reflection picture of the tubules (extensions of the picture: $\approx 90 \times 90 \mu\text{m}$).

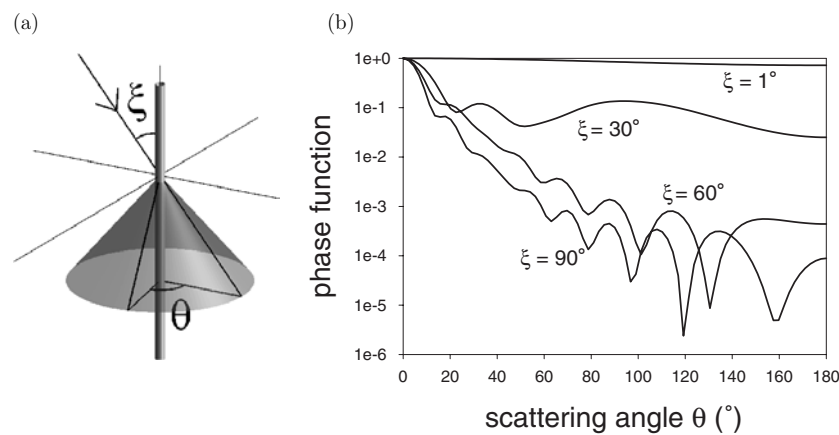


Figure 2. (a) Cone of scattered light formed by illuminating an infinitely long cylinder with incidence angle ξ . (b) Phase function for different ξ -values.

using a laser scanning microscope (LSM). Figure 1(b) shows a reflection measurement. It can be seen that the tubules have a cylindrical form with approximately parallel directions. The diameter of the tubules is about $2 \mu\text{m}$. Thus, the scattering by a single tubule can be approximately calculated by solving the Maxwell equations for an oblique incident plane electromagnetic wave that is scattered by an infinite long cylinder (Yousif and Boutros 1992, Zijp and ten Bosch 1993). The angle between the incident direction of the photons and the cylinder axis is termed ξ . The calculations show that the scattered photons form a cone with the cylinder as the axis of the cone having a half angle ξ (Bohren and Huffman 1983) (see figure 2(a)). This means that for an incidence angle of $\xi = 90^\circ$ the cone turns into a plane perpendicular to the direction of the cylinder. One has to emphasize that there is no scattering in other directions. The intensity distribution along the cone is given in figure 2(b) for a cylinder representing a tubule. The calculations were done for unpolarized light and for four different ξ -values. The following parameters were used: the diameter of the cylinder $d = 2 \mu\text{m}$, the refractive index of the cylinder $n_{\text{in}} = 1.33$ (the contents of the tubules consist mainly of water) and of the tissue surrounding the cylinder $n_{\text{out}} = 1.52$ (Zijp and ten Bosch 1993), the wavelength of the incident light $\lambda = (633/n_{\text{out}}) \text{ nm}$. From the above parameters only n_{out} is not readily obtained; however, uncertainties in this quantity do not strongly influence the

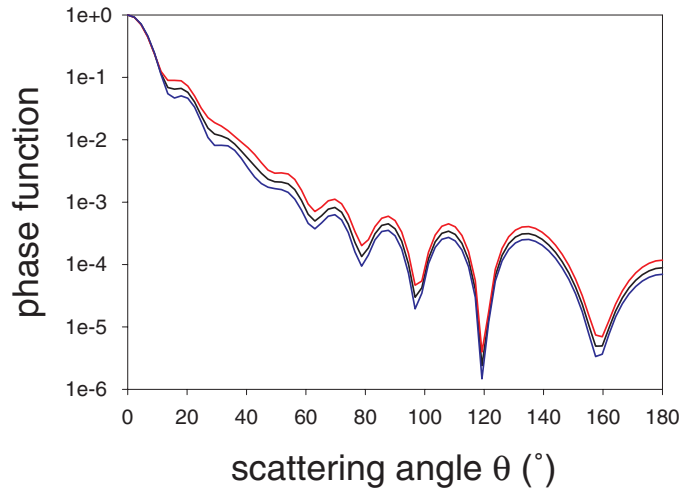


Figure 3. Phase function for different refraction indices outside the cylinder $n_{\text{out}} = 1.50$ (lower curve), 1.52 (middle curve), 1.54 (upper curve). The other parameters are $d = 2 \mu\text{m}$, $n_{\text{in}} = 1.33$, $\lambda = (633/n_{\text{out}}) \text{ nm}$.

results. Figure 3 shows that the phase functions for $\xi = 90^\circ$ and three different refractive indices ($n_{\text{out}} = 1.50, 1.52, 1.54$) are very similar.

In order to calculate the light propagation through a dentin slab having a given concentration of tubules, we programmed a Monte Carlo simulation code, which applied the results of the scattering by a single cylinder and considered multi-scattering. In detail, after launching a photon into the dentin slab, the incidence angle ξ between the direction of the photon and the cylinder was calculated. Then, the ‘single cylinder’ phase function for this ξ -value and the scattering coefficient were used to compute the scattering angle and the scattering length. Because the scattering possibilities are restricted to a cone, only the θ -angle (see figure 2(a)) has to be computed. The scattering coefficient μ_s was calculated using

$$\mu_s = Q_{\text{sca}} d c_A \quad (1)$$

where Q_{sca} is the scattering efficiency obtained from the ‘single scattering’ calculation and $c_A = 4.5 \times 10^4 \text{ mm}^{-2}$ is a typical value for the density of dental tubules (number per area) (Zijp and ten Bosch 1993). We note that both Q_{sca} and μ_s depend on ξ . For $\xi = 90^\circ$ and the above-mentioned cylinder properties we get $Q_{\text{sca}} = 3.15$ from the ‘single cylinder’ calculations. Thus, the scattering coefficient is 284 mm^{-1} . Therefore, even for thin dentin slabs ($20 \mu\text{m}$) we have to consider multi-scattered photons. The absorption coefficient was assumed to be zero, because it is much smaller than the scattering coefficient and, thus, does not noticeably influence the results. After having computed the first scattering interaction the calculations were repeated until the photon was transmitted or remitted considering the Fresnel equations at the slab boundaries. The location, where the transmitted photons are incident onto the screen (see next section), was scored. In the Monte Carlo simulations we did not consider the polarization effects.

To compare the theory with goniometric experiments, we prepared dentin slabs, which were cut from extracted human teeth by using a diamond saw. Two samples were ground and polished to a thickness of about $20 \mu\text{m}$. The tubules were oriented either parallel or perpendicular to the slab surface. In addition, a sample with a thickness of $200 \mu\text{m}$ was made, the tubules of which had an angle of 30° relative to the sample surface. The samples were

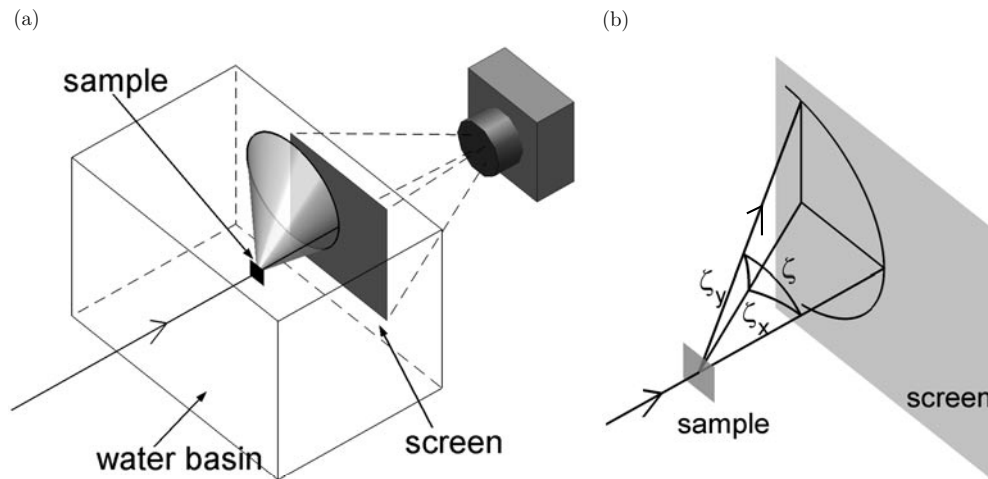


Figure 4. (a) Experimental set-up for measuring the angularly resolved reflectance. (b) Definition of the angles ζ , ζ_x and ζ_y .

illuminated by an unpolarized He–Ne laser ($\lambda = 543, 633 \text{ nm}$). The transmitted (scattered and unscattered) light was incident upon a screen, which was imaged onto a CCD camera (see figure 4(a)). The distance between the slab and the screen was much larger than the area at the slab boundary where the photons were transmitted. Thus, the experiment delivers two-dimensional angularly resolved, i.e. goniometric, scattering data. The dentin sample was surrounded by water to simulate the natural environment of the teeth.

Figure 5 shows the Monte Carlo simulations (left column) and the measured scattering pattern (right column) obtained for a slab that was cut parallel to the direction of the tubules (thickness: $20 \mu\text{m}$). In order to illustrate the involved angles the intensity of the scattering pattern is shown versus the angle ζ formed between the scattered photon's direction and the direction normal to the screen (see figure 4(b)). By rotating the dentin sample three different incidence angles of the laser beam relative to the tubules' direction were investigated. A Gaussian distribution with a standard deviation of 4° was assumed for the directions of the tubules in the calculations (compare figure 1(b)). The theoretical and experimental results show the same main features of the transmitted light. At $\xi = 80^\circ$ the scattering pattern has a slightly curved form, which is more pronounced for $\xi = 60^\circ$ and, especially, for $\xi = 40^\circ$. These results can be qualitatively understood considering the scattering by a single cylinder (see figure 2(a)). In principle, they are caused by the intersection of the scattering cones with the plane screen.

Figure 6 shows the comparison of the Monte Carlo simulations (left column) and the experiments (right column) for the slab having a thickness of $200 \mu\text{m}$, the tubules of which had an angle of 30° relative to the sample surface. Two measurements were performed. First, the incident light was perpendicular to the sample surface. Second, the sample was rotated until the curved form of the scattering pattern disappeared. In the Monte Carlo simulations the same optical properties for the thin slabs were used, but the standard deviation for the Gaussian distribution of the direction of the tubules was increased to 7° , because in the thicker sample larger differences in the tubules' directions are expected. The simulations show the main features of the experimental scattering patterns. Although the anisotropy is not as large as for the thin slab, the transmitted light from the $200 \mu\text{m}$ thick sample still shows a pronounced anisotropic light propagation.

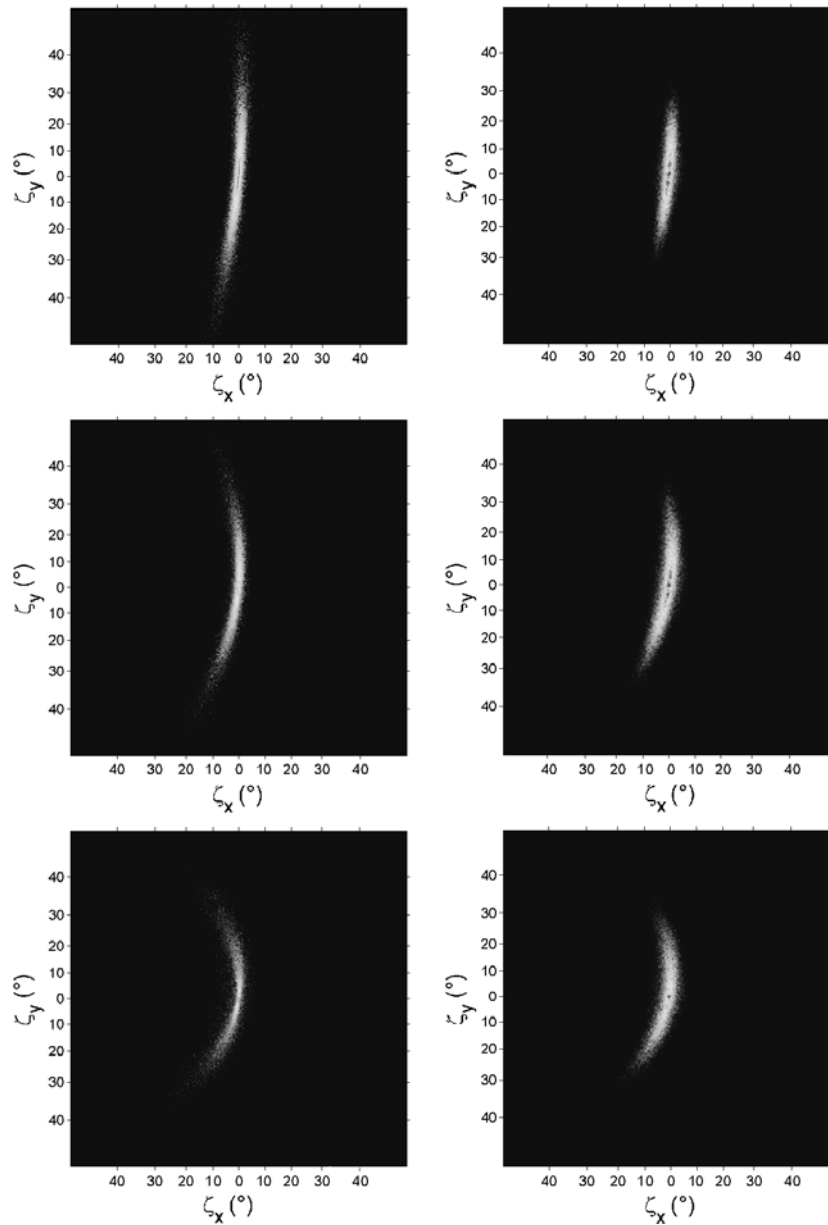


Figure 5. Calculated (left column) and measured (right column) two-dimensional scattering pattern transmitted through a dentin slab (thickness: $20\ \mu\text{m}$) (upper row: $\xi = 80^\circ$, middle row: $\xi = 60^\circ$, lower row: $\xi = 40^\circ$). The parameters used in the calculations were: $d = 2\ \mu\text{m}$, $n_{\text{in}} = 1.33$, $n_{\text{out}} = 1.52$, $\lambda = (633/n_{\text{out}})\ \text{nm}$, n outside the dentin slab = 1.33, density of tubules = $4.5 \times 10^4\ \text{mm}^{-2}$.

In addition to these scattering patterns, intensity peaks at angle ζ are measured with the goniometric experiments if the dental slabs are thin and the concentration of the tubules is small. In the literature, these peaks were considered to be caused by diffraction (Zijp and ten Bosch 1991, 1993, Fried *et al* 1995), but only in Zijp and ten Bosch (1993) a quantitative analysis

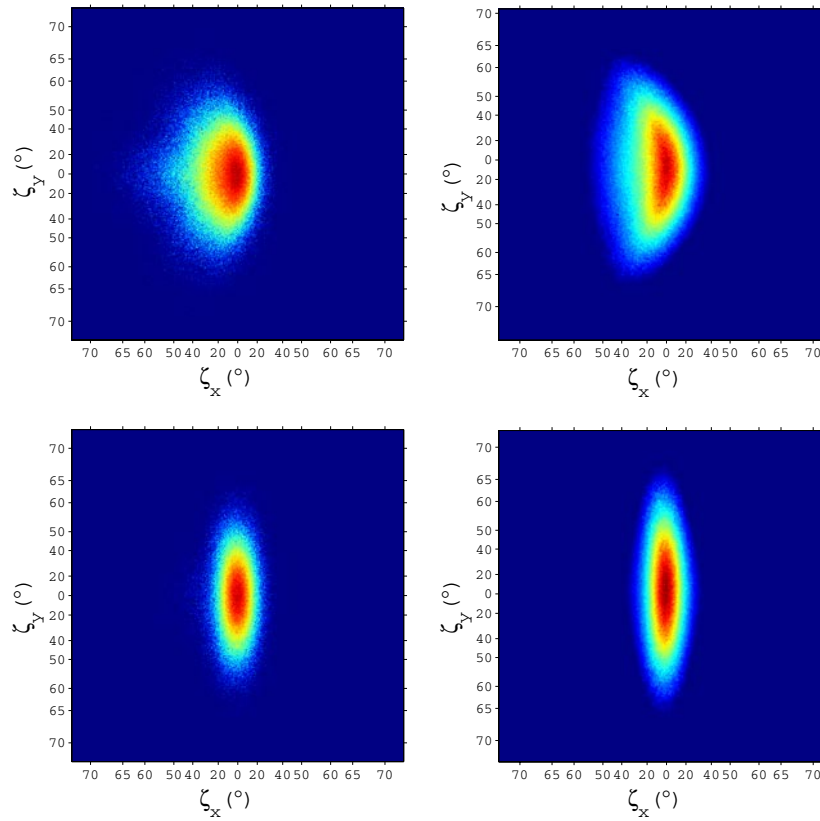


Figure 6. Calculated (left column) and measured (right column) two-dimensional scattering pattern transmitted through a dentin slab (thickness: $200\ \mu\text{m}$), the tubules of which had an angle of 30° relative to the sample surface (upper row: incident beam perpendicular to surface; lower row: oblique incident beam). The parameters used in the calculations were: $d = 2\ \mu\text{m}$, $n_{\text{in}} = 1.33$, $n_{\text{out}} = 1.52$, $\lambda = (633/n_{\text{out}})\ \text{nm}$, n outside the dentin slab = 1.33, density of tubules = $4.5 \times 10^4\ \text{mm}^{-2}$.

was performed. They introduced two approximations; first, they assumed a one-dimensional distribution of tubules and, second, they used a fixed axis-to-axis distance between the tubules having a certain standard deviation. For a more realistic analysis we used the set-up in figure 4(a) to measure the angularly resolved transmission from a slab that was cut perpendicular to the direction of the tubules. The beam was incident, perpendicular to the slab (same direction as the tubules). The thickness of the slab was $20\ \mu\text{m}$.

Figure 7(b) shows that the obtained scattering pattern has a ring structure. From the illumination site also a light microscopy picture was taken (see figure 7(a)). Then, we calculated whether this distribution of the tubules can cause a scattering pattern as seen in figure 7(b). We regarded each tubule as a scattering centre and determined the positions of the tubules in figure 7(a). The scattered waves from all tubules were summed, squared and time-averaged for each direction to obtain the scattered intensity. Finally, the intensity was multiplied by the diffraction function of a circular hole having a mean diameter of the tubules (compare figure 7(a)). The results were azimuthally averaged and are shown in figure 7(c) for $\lambda = 633\ \text{nm}$ and $543\ \text{nm}$. Also shown are the azimuthally averaged intensity curves of the measured data. The angles of the intensity peak obtained from the measurements

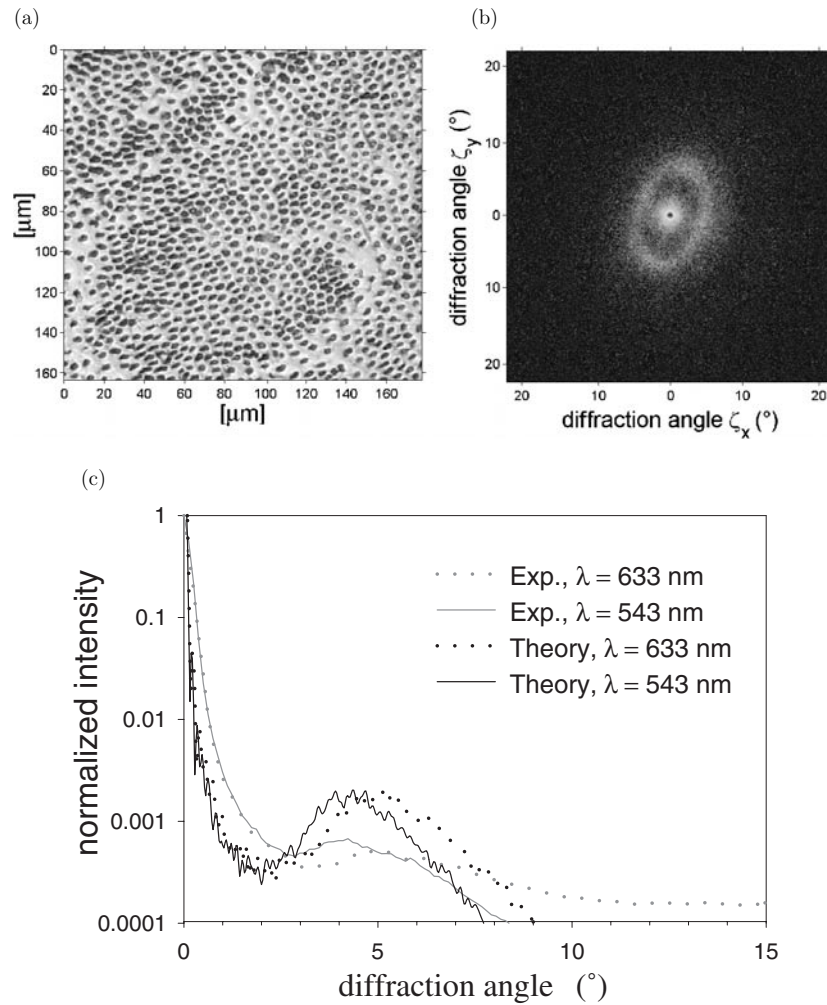


Figure 7. Diffraction by a thin dentin slab. (a) Light microscopy picture of the tubules. (The dentin slab was cut perpendicular to the tubules.) (b) Measured diffraction pattern. (c) Radial intensity distribution.

are $\zeta = 4.1^\circ$ and 5.3° , and the theoretical values are $\zeta = 4.3^\circ$ and 5.1° for $\lambda = 543$ and 633 nm, respectively. From this we get for the average distance of the tubules $d_t = 5.7 \mu\text{m}$ (543 nm) and $5.2 \mu\text{m}$ (633 nm) for the experiment and $d_t = 5.4 \mu\text{m}$ (543 nm) and $5.4 \mu\text{m}$ (633 nm) for the theory using the formula for diffraction by a grating. In addition, we calculated the average distance of the tubules from figure 7(a) as $d_t = 5.4 \mu\text{m}$. Thus, it is confirmed that the scattering peaks are indeed caused by diffraction.

In summary, we showed that the light propagation in dentin can be explained by its microstructure. Scatterers other than the tubules, for example the mineral crystals, can be easily integrated in the model by adding an isotropic component to the phase function. For the calculation of light propagation in larger dentin volumes solely the three-dimensional distribution of the tubules has to be provided for the Monte Carlo simulations. It was also found that the light propagation in dentin is considerably anisotropic. (This should not be confused with an anisotropic phase function (Kienle *et al* 2001). In dentin the phase function depends,

additionally, on the incident angle.) In the literature the anisotropic light scattering in dentin is documented; however, it was argued that it is caused by diffraction (Zijp and ten Bosch 1993), by waveguide effects (Altshuler 1995) or was not explained (Fried *et al* 1995). We showed, however, that it is caused by scattering by the cylindrically shaped tubules. For tissue other than dentin Nickell *et al* (2000) described an anisotropic model for light propagation in skin. They used a simple heuristic formula for an angle-dependent scattering coefficient to calculate the light propagation in skin using Monte Carlo simulations.

As a conclusion from our study the isotropic models that are usually applied to describe the light propagation of the biological tissue are not valid for dentin. For example, if the optical properties of a dentin slab, that is cut with an angle larger than 45° relative to the directions of the tubules, are measured with the standard method of the integrating spheres, one obtains no diffuse remission, because all light is scattered in the forward half-space. Thus, it is concluded that the scattering coefficient of the highly scattering dentin is zero.

In addition, for an anisotropic tissue it is not sufficient to perform an angle-resolved measurement in one plane and assume rotational symmetry to obtain the phase function of the considered tissue as was normally assumed in the literature. Finally, we want to emphasize that the model presented in this study is not restricted to dentin. It can be used for all tissue types, whose anisotropic light propagation is caused by cylindrical structures like collagen fibres or myofibrils (Zijp and ten Bosch 1998, Marquez *et al* 1998).

References

- Altshuler G B 1995 Optical model of the tissues of the human tooth *J. Opt. Technol.* **62** 516–20
- Backman V *et al* 2000 Detection of preinvasive cancer cells *Nature* **406** 35–6
- Beuthan J, Minet O, Helfmann J, Herrig M and Müller G 1996 The spatial variation of the refractive index in biological cells *Phys. Med. Biol.* **41** 369–82
- Bohren C F and Huffman D R 1983 *Absorption and Scattering of Light by Small Particles* (New York: Wiley)
- Drezek R, Dunn A and Richards-Kortum R 1999 Light scattering from cells: finite-difference time-domain simulations and goniometric measurements *Appl. Opt.* **38** 3651–63
- Fried D, Glens R E, Featherstone J D B and Seka W 1995 Nature of light scattering in dental enamel and dentin at visible and near-infrared wavelengths *Appl. Opt.* **34** 1278–85
- Kienle A, Forster F K and Hibst R 2001 Influence of the phase function on determination of the optical properties of biological tissue by spatially resolved reflectance *Opt. Lett.* **26** 1571–3
- Marquez G, Wang L V, Lin S-P, Schwartz J A and Thomsen S L 1998 Anisotropy in the absorption and scattering spectra of chicken breast tissue *Appl. Opt.* **37** 798–804
- Mourant J R, Johnson T M, Carpenter S, Guerra A, Aida T and Freyer J P 2002 Polarized angular dependent spectroscopy of epithelial cells and cell nuclei to determine the size scale of scattering structure *J. Biomed. Opt.* **7** 378–87
- Nickell S, Hermann M, Essenpreis M, Farrell T J, Krämer U and Patterson M S 2000 Anisotropy of light propagation in human skin *Phys. Med. Biol.* **45** 2873–86
- Perelman L T *et al* 1999 Observation of periodic fine structure in reflectance from biological tissue: a new technique for measuring nuclear size distribution *Phys. Rev. Lett.* **80** 627–30
- Yousif H A and Boutros E 1992 A FORTRAN code for the scattering of EM plane waves by an infinitely long cylinder at oblique incidence *Comput. Phys. Commun.* **69** 406–14
- Zijp J R and ten Bosch J J 1991 Angular dependence of He–Ne-laser light scattering by bovine and human dentine *Arch. Oral Biol.* **36** 283–9
- Zijp J R and ten Bosch J J 1993 Theoretical model for the scattering of light by dentin and comparison with measurements *Appl. Opt.* **32** 411–5
- Zijp J R and ten Bosch J J 1998 Optical properties of bovine muscle tissue *in vitro*: a comparison of methods *Phys. Med. Biol.* **43** 3065–81